RAA 2019 Vol. **19** No. **1**, 4(12pp) doi: 10.1088/1674–4527/19/1/4

http://www.raa-journal.org *http://iopscience.iop.org/raa*

Research in Astronomy and Astrophysics

Searching for exoplanets with *HEPS*: I. detection probability of Earth-like planets in multiple systems

Zhou-Yi Yu[1], Hui-Gen Liu[1], Ji-Lin Zhou[1], Dong-Hong Wu[1], Ming Yang[1], Songhu Wang[2⋆], Hui Zhang[1], Zi Zhu[1] and Jia-Cheng Liu[1]

[1] School of Astronomy and Space Science, Key Laboratory of Modern Astronomy and Astrophysics in Ministry of Education, Nanjing University, Nanjing 210093, China; *huigen@nju.edu.cn, zhoujl@nju.edu.cn*

[2] Department of Astronomy, Yale University, New Haven, CT 06511, USA

Received 2018 March 29; accepted 2018 July 7

Abstract The astrometry method has great advantages in searching for exoplanets in the habitable zone around solar-like stars. However, the presence of multiple planets may cause a problem with degeneracy when trying to compute accurate planet parameters from observation data and reduce detectability. The degeneracy problem is extremely critical, especially in a space mission which has limited observation time and cadence. In this series of papers, we study the detectability of habitable Earth-mass planets in different types of multi-planet systems, aiming to find the most favorable targets for the potential space mission–*Habitable ExoPlanet Survey* (*HEPS*). In the first paper, we present an algorithm to find planets in the habitable zone around solar-like stars using astrometry. We find the detectability can be well described by planets' signal-to-noise ratio (SNR) and a defined parameter $S = M_2/(T_1 - T_2)^2$, where M_2 and T_2 are the mass and period of the second planet, respectively. T_1 is the period of the planet in the habitable zone. The parameter S represents the influence of planetary architectures. We fit the detectability as a function of both the SNR of the planet in the habitable zone and the parameter S. An Earth-like planet in a habitable zone is harder to detect (with detectability $P_{\rm HP} < 80\%$) in a system with a hot Jupiter or warm Jupiter (within 2 AU), in which the parameter S is large. These results can be used in target selections and to determine the priority of target stars for *HEPS*, especially when we select and rank nearby planet hosts with a single planet.

Key words: astrometry — stars: planetary systems — planets and satellites: detection — methods: numerical

1 INTRODUCTION

Finding habitable planets has become one of the most fascinating topics for exoplanet hunters. To date, 16 exoplanets have already been found in conservative habitable zones (HZs)[1]. Most planets are detected by the transiting or radial velocity methods, as shown in Table 1. Both methods prefer to detect planets close to host stars, because these planets cause a larger radial velocity in their host stars or have larger chances to transit the host stars. Planets with a long period, e.g. planets in the HZ around solar-like stars, are not easy to detect via transiting or radial velocity methods. However, planets in HZs may be common. Burke et al. (2015) estimate the terrestrial planet occurrence rate according to the *Kepler* GK dwarf sample, and obtain that each FGK star has 0.1 planet with a period between 300 and 700 d, and a radius between 0.75 and 2 Earth radius.

As with other indirect methods, astrometry measures the stellar motion projected on the celestial plane and has some advantages compared with current popular methods. Planets with larger semi-major axes cause larger motions in their host stars, which is contrary to the radial velocity method. Compared with the transiting method, there is no limitation on the inclination of the planets via as-

⋆ 51 Pegasi b Fellow

[1] based on the NASA Exoplanet archive.

Table 1 Sixteen exoplanets in HZs (from *https://exoplanetarchive.ipac.caltech.edu/index.html*). The columns include the planet name, period, equilibrium temperature, radius, total number of planets around the host star and detection method, from left to right respectively.

Planet Name	P (d)	$T_{\rm eq}$ (K)	$R_{\rm p}(R_\oplus)$	PN	D (pc)	Spectral	Method
Kepler-62e	122.39	270	1.61	5	368	K2 V	Transit
Kepler-61b	59.88	273	2.15	1	314	K7 V	Transit
PH2 b	282.53	281	10.12	1	346	–	Transit
K2-3 d	44.56	282	1.51	3	–	M0 V	Transit
Kepler-1653b	140.25	284	2.17	1	755	–	Transit
TRAPPIST-1d	4.05	288	0.772	7	12.1	–	Transit
Kepler-69c	242.46	299	1.71	2	584	G4 V	Transit
Ross 128 b	9.87	301	–	1	3.38	M4	Radial Velocity
K2-9 b	18.45	314	2.25	1	–	M2.5 V	Transit
HD 42618 b	149.61	337	–	1	23.5	G4 V	Radial Velocity
TRAPPIST-1c	2.42	342	1.056	7	12.1	–	Transit
K2-3 c	24.64	344	1.85	3	–	M0 V	Transit
GJ 3021 b	133.71	350	–	1	17.62	G6 V	Radial Velocity
HD 192310 b	74.72	355	–	2	8.82	K3 V	Radial Velocity
K2-18 c	8.96	363	–	2	34	M2.5 V	Radial Velocity
CFBDSIR J145829+101343 b	10037.50	370	–	1	23.1	–	Imaging

trometry. Thus astrometry is a proper method to detect planets in the HZ around nearby solar-like stars, although there have been no exoplanets discovered by astrometry to date. Another important advantage for astrometry is that the planet's mass and all the six orbital elements can be obtained simultaneously, e.g., astrometry has already been used to determine the masses of celestial bodies and associated orbits in binary systems, such as the mass of the black hole at the center of the Milky Way (Schödel et al. 2002). Although transit timing variations (TTV) can be used to calculate the planet mass, it usually takes a long time (Miralda-Escudé 2002; Xie 2013; Yang et al. 2013). In most situations, we need to combine radial velocity with transiting to calculate the planet mass, e.g. like the case HAT-P-1 b (Bakos et al. 2007).

However, the detection of planets' astrometric signals requires very high precision. For example, assuming there is another solar system 10 pc away, the astrometric signal of a star induced by Earth is around $0.3\,\mu$as. Such a precision has not been achieved, even by the most recent satellite, *Gaia*. The highest astrometric precision of *Gaia* is 10.6 µas, for a star which has G magnitude < 12 (Perryman et al. 2014). Under such a precision, they estimated that 21 000 high-mass ($1 - 16\,M_{\rm J}$) (Jupiter mass) planets out to ~ 500 pc should be detected during the *Gaia* mission in 5 yr. However, detecting Earth-like planets in the HZ requires a sub-microarcsecond precision. Some space astrometry telescopes have been proposed, e.g., *SIM* (Unwin et al. 2008) and *NEAT* (Malbet et al. 2012). The plan for both satellites is to achieve a sub-microarcsecond astrometric precision and detect Earth-like planets in their HZs, which is the ongoing major scientific goal. However, these projects have either been postponed or canceled.

Habitable ExoPlanet Survey (HEPS) is a potential space mission proposed by Chinese scientists, which used to be called the *Searching for Terrestrial Exo-Planet* (*STEP*) satellite (Chen et al. 2013). It is comprised of a 1.5 meter aperture space telescope at the Sun-Earth 2nd Lagrange point L_2. With a plan to search for ~ 100 targets within 10 pc during its 5-yr lifetime, it aims to do a survey of Earth-like planets in the HZ around these stars, including 70 FGK stars (Henry et al. 2018). Some interesting M stars like Proxima (Anglada-Escudé et al. 2016; Liu et al. 2018) and planet hosts further than 10 pc are also selected for *HEPS*. The designed astrometric precision of *HEPS* is 1 µas for stars with V magnitude $= 8$, which is comparable to the precision mentioned by projects *NEAT* and *SIM*. The preliminary observational strategy of *HEPS* is to measure each target 50 times in 5 yr.

Due to the limitation of the space mission's lifetime, we need to rank the observation priority of target stars to maximize the scientific fruits of the *HEPS* mission. The priority of target stars depends on lots of aspects, e.g. the scientific motivation, the signal-to-noise ratio (SNR), the distance, etc. The most important one is the detection probability of an Earth-like planet in an HZ. Previous works have investigated the probability of detecting planets with 1-µas precision (Perryman et al. 2014; Malbet et al. 2012). Their works mainly focus on single-planet systems, and find the major factor which influences the detection probability is the SNR.

However, Udry et al. (2017) show that multi-planetary systems are common and they found 20 exoplanets in eight systems. Some multi-planet systems, like TRAPPIST-1 (Gillon et al. 2017), have many planets in their systems. The identification of planet orbits in a multi-planet system is more complex than that in a single-planet system, because of the larger fitting parameter space, i.e. there are five astrometric parameters for the host star, and seven parameters for each planet. Even for a two-planet system, there are 19 parameters that need to be fitted. It is similar with radial velocity fitting in multi-planet systems. Different models of single or multiple planets may produce different local minima in the searching algorithm, which thus results in different fitted orbit parameters (Wittenmyer et al. 2013; Wright & Howard 2009). This is the degeneracy problem in the orbit fitting procedure. The problem is more severe for the detection of Earth-like planets in the HZ, because the fitting residual of the other planets, which depends on SNR, may contaminate the small signal of an Earth-like planet in the HZ. The influence from other planets in the same system was not investigated in detail, although it is very important for detecting an Earth-like planet.

In this paper, considering the proper motions and parallaxes of host stars, we use a linear model to simulate their astrometric motions. We also assume an Earth-like planet in the HZ, with a companion planet having different masses and locations. By using the commonly adopted Levenberg–Marquardt (LM) algorithm of planet-searching (Wright & Howard 2009), we investigate the detection probability of an HZ planet. We find the fitting accuracy of orbital elements, especially the eccentricity and inclination, vary in different systems, even when the planets have the same SNR. We find the SNR of the planet is not good enough to describe the astrometric detectability in multi-planet systems, and we propose a new parameter to give a more precise description of detectability for habitable planets in these systems.

The paper is arranged as follows: In Section 2, we present the method we adopted in simulating the astrometry data. In Section 3, we estimate the probability of detecting Earth-like planets in the HZ in some typical systems. The influences of SNR and orbital configurations are investigated in detail. Conclusions and discussions are made in Section 4.

2 ASTROMETRY MODEL AND FITTING PROCESSES

2.1 The Simulation of Stellar Astrometric Motion

The astrometry method is able to measure stellar motions projected on the celestial plane. Due to the gravity of exoplanets, the host star orbits the barycenter of the star and planets. Besides, the star also has proper motion, perspective acceleration and parallax. Stellar motions in the right ascension α and declination δ directions can be expressed as

$$
\begin{aligned}
\alpha_t \; = \; & \alpha_0 + \mu_\alpha^* t + (\mu_\alpha^* \mu_\delta \tan\delta - \mu_\alpha^* \pi V_{\rm r})\, t^2 \\
& + \pi\,(-y\cos\alpha + x\sin\alpha)\sec\delta \\
& - \frac{1}{\rm c}\,(\dot{x}\cos\alpha\sin\delta - \dot{y}\cos\alpha\sec\delta) \ , \qquad (1) \\
\delta_t \; = \; & \delta_0 + \mu_\delta t - \left(\frac{1}{2}{\mu_\alpha^*}^2 \sin\delta\cos\delta + \mu_\delta \pi V_{\rm r}\right) t^2 \\
& + \pi\,(x\cos\alpha\sin\delta + y\sin\alpha\cos\delta - z\cos\delta) \\
& - \frac{1}{\rm c}\,(\dot{x}\cos\alpha\sin\delta + \dot{y}\sin\alpha\sin\delta - \dot{z}\cos\delta) \ , \qquad (2)
\end{aligned}
$$

where $\alpha_{\rm t}$ and $\delta_{\rm t}$ are the stellar position at time t in the right ascension and declination respectively. α_0 and δ_0 are the stellar position at $t = 0$. $\mu_\alpha^* = \mu_\alpha \cos(\delta)$ and μ_δ are the proper motions in the right ascension and declination directions, respectively. π is the parallax of the star and $V_{\rm r}$ is the radial velocity of the star. (x, y, z) and $(\dot{x}, \dot{y}, \dot{z})$ are the satellite's position and velocity relative to the barycenter of the solar system respectively. The third term containing t^2 is the acceleration of the stellar proper motion. The last two terms are annual parallax and aberration, respectively. The value of annual aberration, which depends on the positions and velocities of stars, is sometimes comparable to the parallax. However, if we know the priori position and velocity of the star and the satellite, we are able to calculate the value of the last two terms. Under a precision of 10–100 µas in the *Gaia* era, the last three terms can be corrected with a precision much less than 1 µas.

Therefore, we choose a simple model of stellar motion, and add the influence of planets during data fitting. We assume we know the exact value of the position and velocity of the satellite at any given time and ignore the acceleration term and annual aberration term. We use X and Y to represent the stellar motion in the right ascension and declination directions respectively. The stellar motions projected to the celestial plane can be simply expressed as

$$X = X_0 + V_x(t - t_0) + P_x/d + \delta_x + \sigma_x \ , \qquad (3)$$

$$Y = Y_0 + V_y(t - t_0) + P_y/d + \delta_y + \sigma_y \ , \qquad (4)$$

where X_0 and Y_0 are offsets, and V_x and V_y are the proper motions of the star in X and Y directions, respectively. P_x and P_y are parallax factors. t is the observation time and the zero point t_0 represents the time of the first measurement. d is the distance between the star and the barycenter of the solar system. δ_x and δ_y are the stellar motions relative to the system barycenter due to the planets. σ_x and

σ_y are the noise we add in the X and Y directions, respectively. In this paper, a Gaussian distribution is adopted to generate the noise in an individual direction randomly. The standard deviations in both directions are the same, with the same mean value of 0. A similar form was also used in other simulations (Perryman et al. 2014; Casertano et al. 2008). We take a linear proper motion model, i.e., the stellar proper motion is unchanged during five years. In our work, the parallax parameters, P_x and P_y, are assumed to be known. Only X_0, Y_0, V_x, V_y, $1/d$ and planets' orbital elements are the parameters which we are going to fit in this work.

An example simulation is shown in Figure 1. The left panel is HD 192310's astrometric motion in the X and Y directions using Equations (3) and (4), respectively. There are 50 positions in five years with constant intervals of 0.1 yr. The stellar distance is 8.91 pc and its proper motion is $V_x = 1241.85\,\mathrm{mas\,yr^{-1}}$ and $V_y = -180.96\,\mathrm{mas\,yr^{-1}}$, according to *Hipparcos* data (van Leeuwen 2007). The proper motion and parallax are much larger than the motion caused by planets.

To estimate astrometric signals of exoplanets, we use A to denote the maximum amplitude of stellar motion caused by a specific planet. The value of A is related to the planet mass M_p, the planet orbital elements, the host star mass M_s and the distance d from us. If we only consider M_p, M_s, d and the semi-major axis of the planet a_p, A can be expressed as follows

$$A \approx 3\left(\frac{M_\mathrm{p}}{1\,M_\oplus}\right)\left(\frac{a_\mathrm{p}}{1\,\mathrm{AU}}\right) \times \left(\frac{M_\mathrm{s}}{1\,M_\odot}\right)^{-1}\left(\frac{d}{1\,\mathrm{pc}}\right)^{-1}\ \mu\mathrm{as}\ . \tag{5}$$

Then we can define the SNR as the signal-to-noise ratio for the detection of each exoplanet. It can be expressed as

$$\mathrm{SNR} = \frac{A}{\sigma}\ , \tag{6}$$

where σ is the standard deviation of the Gaussian distribution we added in the X and Y directions, and we set $\sigma = \sigma_x = \sigma_y$ in Equation (3).

2.2 Fitting Program

To find a planet in the simulated data based on Equations (3) and (4), we will introduce the fitting process in this section. To fit the planet parameters, we follow fitting processes step by step, i.e.,

Step 1: Estimate the initial values of the offset point X_0, Y_0, the proper motion V_x, V_y and $1/d$, by linear fitting.

Step 2: Use Generalized Lomb-Scargle (GLS) (Zechmeister & Kürster 2009) in PyAstronomy[2] to find the periodic signals in residuals after the linear fitting in Step 1. The residuals in the X and Y axes should be analyzed separately. Comparing the strongest peaks in both periodograms, the period with the smaller false alarm probability (FAP) is adopted.

Step 3: Using the method of fitting single planet orbital elements, we fit the Thiele-Innes elements (Wright & Howard 2009) directly, via the LM algorithm (Marquardt 1963). All the parameters are fitted simultaneously, including parameters of previously detected planets and parameters of the host star. In order to avoid local minima, we scan the initial eccentricity and mean anomaly, which are the nonlinear fitting parameters using Thiele-Innes elements, to find the best fitted parameters.

Step 4: Subtracting the signal of the fitted planet in Step 3, we repeat Steps 1–3, until the FAPs in both X and Y directions are greater than a threshold of 1%, i.e., there are no significant periodic signals in the residuals and the fitting processes are completed.

Note that, in Step 2, periods in the X and Y directions are nearly the same in all our simulations. However, if the periods are different, the period with smaller FAP< 0.01 is adopted as the initial value. While iterating Step 4, all the parameters of both the planets and the stars are refitted to obtain a more accurate result with smaller residuals.

To test the efficiency of our program, we use the fitting program to fit the planets in HD 192310, as mentioned in the previous section. We choose this planetary system because the host star mass is close to the Sun and its distance is within 10 pc. The host star has a mass of $0.8\,M_\odot$ (van Leeuwen 2007) and its distance is 8.91 pc (van Leeuwen 2007), which is suitable for *HEPS* detection. Two planets, HD 192310 b and c, have already been found (Howard et al. 2011; Pepe et al. 2011). However, these two planets are not in the HZ of the system. To test our program for finding planets in the HZ, we add a test planet, HD 192310 d, into the system. The masses, periods and eccentricities of HD 192310 b and c are based on the values in Pepe et al. (2011). The inclination was not determined. We assume they have a mean value of 45 degrees. We define the inclination as the angle between the line of sight and the perpendicular line of the planet's orbital plane. Other orbital elements are generated randomly in our test. The test planet, HD 192310 d, has a mass of 10 Earth masses and is located at 0.8 AU in the HZ of the system.

[2] *https://github.com/sczesla/PyAstronomy*

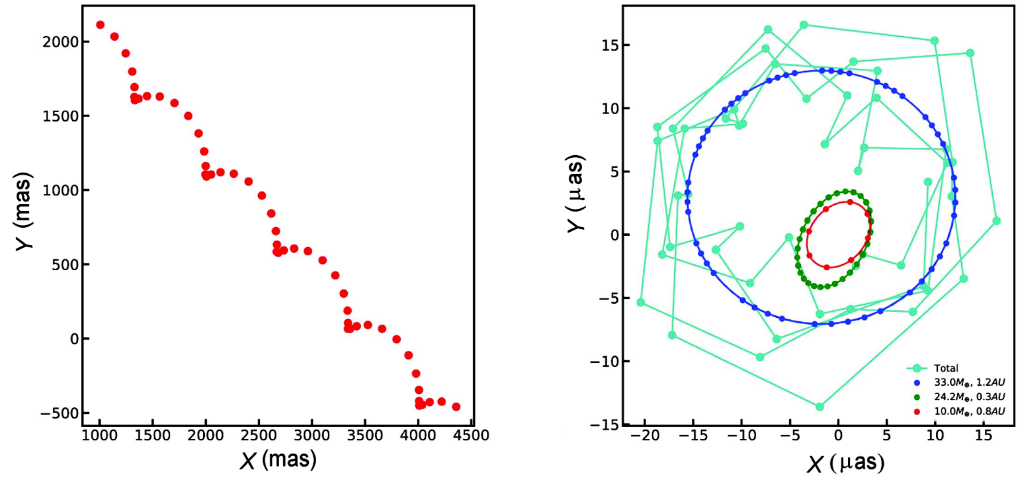

Fig. 1 The simulation of HD 192310's astrometric motion based on Eqs. (3) and (4). The left panel includes total proper motion and parallax. The right panel shows the motion excluding the proper motion and parallax. The *cyan line* is the total motion of the host star including a white noise of 0.4 µas. The *blue*, *green* and *red lines* represent stellar motion due to planets HD 192310 b, c and d, respectively. The planet HD 192310 d is a virtual planet we put into the system to test our program for finding an HZ planet.

The HZ of the system is calculated based on Kopparapu et al. (2013). The detailed parameters of the planets are listed in the upper part of Table 2. δ_x and δ_y are generated via RKF78 integrator, a Fortran subroutine developed by us according to Fehlberg (1968) and Montenbruck & Gill (2012). The astrometry noise we adopt here is based on a simple Poisson noise model, i.e., a star with a V-band magnitude of 8 has a typical uncertainty of 1 µas. Brighter stars have larger photon flux, leading to a smaller uncertainty, which is $10^{0.4*(V-8)}$ µas. V is the magnitude of the target star in the V-band. In the case of HD 192310, both σ_x and σ_y follow a Gaussian distribution, with the same deviation, ~ 0.40 µas. The noise is smaller than the typical noise of $\sim$1 µas for planets in an HZ, because for bright stars, more measurements can be made to improve astrometric precision. The right panel of Figure 1 shows the stellar astrometric motion caused by the planets. The blue, green and red circles represent the stellar motion caused by planets c and b, and test planet d respectively. The cyan line shows the combination of all three motions caused by planets and the noises.

After finishing our fitting program, three planets are detected. Brief results of every fitting iteration are shown in Figure 2. The left panels show the folded phase of astrometry signals after removing the fitted proper motion and parallax. Different colors represent different directions. The period is based on the periodic signals found in the periodogram at each iteration, which in the right panels of Figure 2. The bottom panels of Figure 2 display the residuals of the fitting and the associated period analysis. The fitting procedure ends when the largest periodic signal's FAP$>$ 1%. The fitting results are listed in the bottom part of Table 2. As we can see, in the triple-planet system, all the masses, semi-major axes and inclinations are fitted well. For the most distant planet c with the largest SNR$>$ 20, both Ω and $\omega + M_0$ are fitted well. However, for the inner planet b and the test planet d with a small signal of about 3 µas, $\omega + M_0$ differs from the real value by over 50 degrees. This demonstrates that the fitting program is efficient for fitting a planet's mass, period, eccentricity and inclination in multi-planet systems.

3 DETECTION PROBABILITY OF AN EARTH-LIKE PLANET IN THE HZ

By using our astrometry signal simulation and fitting program, we investigate the detection probabilities of Earth-like planets in an HZ in different types of two-planet systems in this section. According to the case of HD 192310 d, though SNR is high enough to detect the planet, the orbital elements obviously differ from the real ones. Well-fitted parameters are significant in finding habitable planets. A planet's habitability depends on its mass and orbital elements (Kopparapu et al. 2013). Beyond the criterion of SNR, we use the detection probability of an Earth-like planet in an HZ (hereafter $P_{\rm HP}$) to evaluate astrometry detection in multi-planet systems. It can be expressed as

$$P_{\rm HP} = \frac{N_{\rm cri}}{N_{\rm sim}} \ , \tag{7}$$

where $N_{\rm sim}$ is the total number of cases we simulated and fitted, while $N_{\rm cri}$ is the number of cases with planet pa-

Table 2 Real and Fitted Parameters of Planets in HD 192310

Name	$M_{\rm p}(M_{\oplus})$	Period (yr)	a (AU)	ecc	inc (deg)	Ω (deg)	ω+ M_0 (deg)
c	32.60	1.43	1.18	0.32	45.86	183.23	322.50
b	23.62	0.20	0.32	0.13	45.63	224.53	151.56
d	10.00	0.80	0.80	0.00	45.90	204.85	291.03
Fitted results							
c	33.11±0.23	1.44±0.001	1.18±0.04	0.34±0.01	46.77±0.48	183.68±0.10	324.38±1.59
b	23.16±0.60	0.20±0.0001	0.32±0.001	0.01±0.05	44.12±2.29	212.89±4.13	232.08±44.71
d	9.64±0.28	0.80±0.002	0.80±0.001	0.04±0.04	45.65±2.37	208.56±3.26	278.03± 51.42

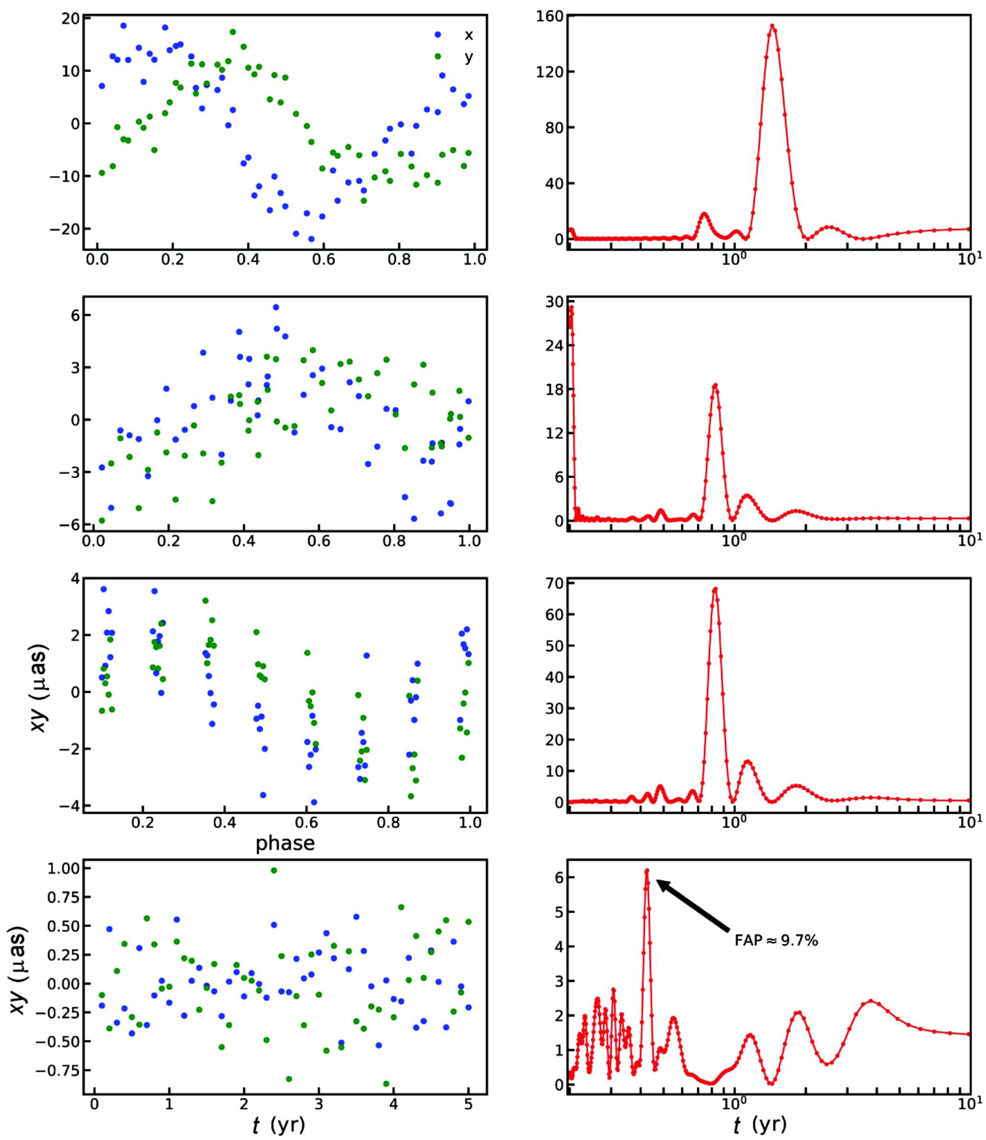

Fig. 2 Fitting processes of planets in HD 192310 via simulated signals with errors of 0.4 μas. The left panel is the folded motions of the host star in the X (*blue dots*) and Y (*green dots*) directions, according to the planet period found in the periodogram. In the right panel, only a periodogram in the X or Y direction with smaller FAP is adopted. The periods of the highest peaks are 1.44 yr, 0.21 yr and 0.80 yr, from top to bottom, respectively. The left bottom panel displays the residuals after three planets are fitted, where we do not fold it into any period. In the periodogram of the final residuals, as shown in the right bottom panel, the FAP of the highest peak is 9.7%, greater than the threshold value 0.01, thus we stop the fitting process.

rameters satisfying the specified criterion. Normally in this paper, $N_{\rm sim} = 50$ which describes the detectability more accurately. The criteria we use here to rank the detection efficiency are

(1) Detect the locations of a planet in the HZ (FAP$< 1\%$). This is the most basic criterion for detecting a habitable planet;
(2) Satisfying Criterion 1, the planet is still an Earth-like planet (fitted mass is 1–17 Earth masses), i.e., the detected planet has a rocky surface;
(3) Satisfying Criterion 2, the planet has a moderate eccentricity (fitted eccentricity $<$0.1), i.e., the well–fitted eccentricities can guarantee that the planet stays in the HZ all the time;
(4) Satisfying Criterion 3, the inclination is well determined (fitted error of inclination $< 5°$), i.e., the most strict criterion to identify planets in an HZ.

These four criteria are sorted by their difficulty in parameter fitting. Criterion 1 is the easiest to achieve while Criterion 4 is hardest. Unwin et al. (2008) found that if a planet is detectable, the SNR of the planet needs to be > 5.4. In the simulation of *NEAT*, Malbet et al. (2012) found that when $\rm SNR = 6$, the FAP is smaller than 1%. However, their results were based on Criteria 1 and 2. They simply assumed $P_{\rm HP} = 1$ for the planets satisfying the requirement of SNR. Considering the eccentricity and inclination, it is more strict to identify planets in HZs because the stellar flux on a planet varies due to the eccentricity, while the inclination between the two planets may increase the eccentricity via the Kozai-Lidov cycle. The angle between the planetary orbit plane and the spin plane is important for the climate of a planet. Similar to Earth, assuming the spin orientation is fixed, the inclination determines the angle between the orbital axis and the spin axis, and leads to a different climate on the planet. Thus, in Criterion 4, if we determine the inclination well, the climate will be constrained better if we assume a fixed spin orientation.

Before showing our results, we test the distribution of the fitting parameters. We fixed the planets in an HZ as 1 Earth mass, period = 1.15 yr, eccentricity = 0.0 and inclination = $45°$. The SNR of the HZ planets is fixed as 5. Another planet is added with random mass from 1 to 100 Earth mass and semi-major axis from 1.5 to 10 AU. The inclination is fixed at 45°. Totally, 200 two-planet systems are adopted and the fitting results of the Earth-like planet in the HZ are shown in Figure 3. The fitting distributions of period, mass, eccentricity and inclination of the planets in the HZ are around the real values we set, demonstrating that our fitting program based on the LM algorithm is able to extract a planet's parameters.

In Section 3.1, we find the requirement for SNR to get a specific $P_{\rm HP}$. We obtain the value of $P_{\rm HP}$ as a function of SNRs. In Section 3.2, we fix the orbital elements of the planets in the HZ to get the same SNR and set the companion planet with different masses and semi-major axes. We calculate the $P_{\rm HP}$ in these systems to investigate which kind of planetary system is more suitable for detecting an Earth-like planet in the HZ. Note in this section, the host stars in all the simulations are solar-mass stars fixed at 10 pc.

3.1 Influence of SNR

To study the dependency of $P_{\rm HP}$ on the SNRs, we set two typical cases: (i) a Jupiter mass planet in a 5 d orbit (Hot-Jupiter case) and (ii) a 100 Earth mass planet at 3 AU (Cold-planet case). The initial eccentricity is set as 0 and the inclination is $45°$. The longitude of ascending node, argument of pericenter and mean anomaly are chosen randomly. In both cases, the habitable planet we are going to detect is 10 Earth masses located at 1.1 AU with an eccentricity = 0.05 and inclination = 45°. We define inclination = 0 as the face-on case while inclination = 90° as the edge-on case. The choice of the location of 1.1 AU is to avoid the influence of annual parallax motion. Due to uncertainty in the distance between the observer and stars, annual parallax will decrease the detection probability of a planet near 1 AU. The longitude of the ascending node, argument of pericenter and mean anomaly of a planet in the HZ are chosen randomly. To investigate the influence of SNR, we set the range of SNR from 0.1 to 30, with the corresponding noise range from 33 to 0.11 μas at a distance of 10 pc. We simulate 50 astrometry measurements in 5 yr, with uniform intervals of 0.1 yr, based on the assumed observation mode of *HEPS*. For each SNR value, we simulate 50 cases in each system and $P_{\rm HP}$ is calculated as the fraction of cases satisfying different criteria.

Figure 4 shows the influence on the $P_{\rm HP}$ of Earth-like planets in the HZ with different SNRs (in the left panel). It shows that the SNR is a crucial factor for detecting planets in the HZ, and suggests that when the SNR is larger than 1, we can detect planets in the HZ with high probability of satisfying Criterion 1, but the parameters of these planets are less reliable. Therefore, it is difficult to determine whether an Earth-like planet in the HZ is habitable or not, due to large uncertainties in planet mass and orbital parameters. When the SNR is improved to > 2, the masses of most planets are determined well. As we enhance the SNR

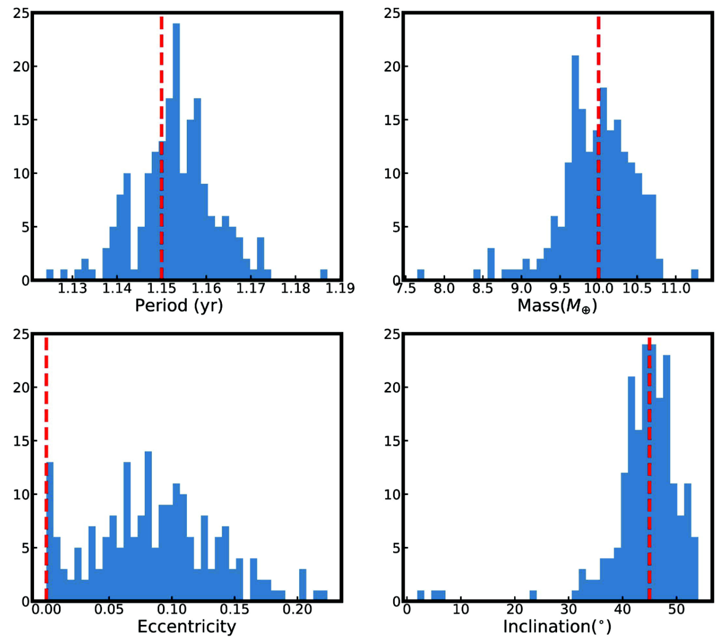

Fig. 3 The sample contains the planetary systems where the HZ planet has an SNR of 5. The *blue bins* demonstrate how the the different parameters of the fitted HZ planets are distributed. The *red dashed lines* indicate the real values of the parameters. These show that the HZ planet is fixed at 10 $M_{\rm Earth}$, period = 1.15, eccentricity = 0.0 and inclination = 45°.

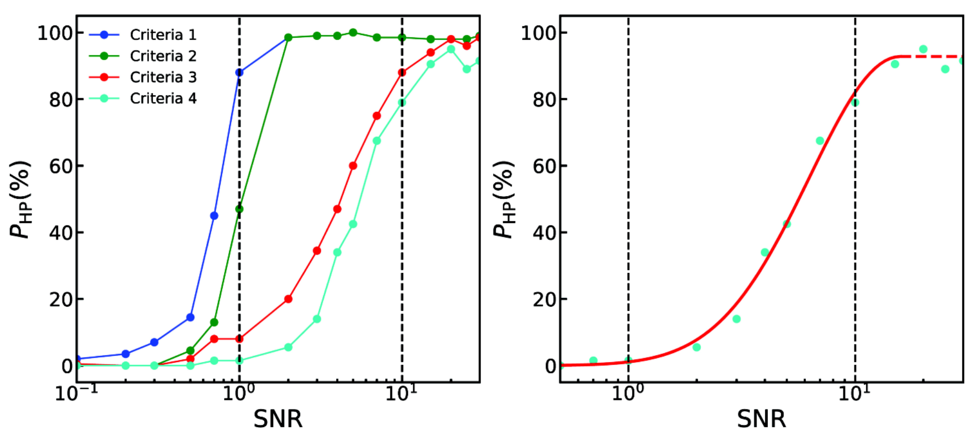

Fig. 4 The SNR of an Earth-like planet in the HZ affects the detection probability $P_{\rm HP}$. The planet is a 10 $M_\oplus$ planet located at 1.1 AU. The astrometric precision varies to obtain different SNRs. The left panel presents the Hot-Jupiter and Cold-planet cases, i.e., a Jupiter mass planet and a 100 Earth mass planet located in 5 d orbits and 3 AU. In both cases, the SNR dominates the detection probability. The *blue*, *green*, *red* and *cyan lines* represent the detection probability using Criteria 1, 2, 3 and 4, respectively. The right panel is the fitting results of $P_{\rm HP}$ based on Criterion 4. The *cyan dots* are $P_{\rm HP}$ based on Criterion 4 with different SNR. The *red line* is the best-fitted curve. Even if SNR > 15.8, $P_{\rm HP}$ assumes a value around 0.928 rather than 1.

to > 10, the eccentricities and inclinations are constrained well, as described in Criteria 3 and 4. The requirement of SNR for Criteria 1 and 2 is much like in single planet systems, but for Criteria 3 and 4, a higher SNR is needed. Using the results based on the strictest case of Criterion 4, the relationship between SNR and $P_{\rm HP}$ can be fitted as

$$P_{\rm HP} = 0.928 \exp\left(-\frac{(K-1.20)^2}{0.325}\right) \ , \qquad (8)$$

$K = \log_{10}$SNR. For SNR > 15.8, $P_{\rm HP}$ reaches the maximum value of –0.928. The fitting line is presented in the right panel of Figure 4.

The requirement of $P_{\rm HP} > 80\%$ based on Criterion 4 is that the SNR of the planets in the HZ should be larger than 10. It is stricter than the requirement based on Criterion 1, which is SNR > 1. However, in the fitting results, even for SNR> 20, the $P_{\rm HP}$ in multi-planet systems cannot exceed 95% in Criterion 3 or 4. This is because of influences from the companion planet. So, the next subsection will study the influences on $P_{\rm HP}$, due to details related to different architectures of planetary.

3.2 Influence of Orbital Architectures

In this section, the parameters of Earth-like planets in the HZ are the same as those set in Section 3.1, i.e. 10 Earth masses at 1.1 AU with eccentricity = 0.05 and inclination = 45°. The SNR of an HZ planet is fixed at 10, i.e. the astrometry uncertainty is fixed at 0.33 μas, to exclude the sensitive influences from the SNR as shown in Section 3.1. We put the companion planet outside the HZ with different masses from 1 to 1000 Earth masses, and different locations, i.e., $1 - 80$ d for inside cases and 1.5 – 100 AU for outside cases, with random eccentricities $<$ 0.05 and inclination $45 \pm 1°$. Thus, as the SNR of the other planet varies a great deal, we investigate the fitting precision of planets in the HZ due to different residuals from the other planet.

Considering our period finding program mentioned in Section 2 and Figure 2, the residuals of the companion planet pollute the period peak of the planet in the HZ. Assuming that the planet signal in the periodogram has a Gaussian profile, and the influence on the planet in the HZ with a period of T_1 is proportional to $e^{-\frac{(T-T_1)^2}{2\sigma^2}}$, T is the period of the companion planet. It is also proportional to the mass of the companion planet. For simplicity, we take a quadratic form of the period into account, and the total effect of the companion planet can be expressed as

$$S = \frac{M}{(T-T_1)^2} \ . \qquad (9)$$

We calculate S for every simulation case and $P_{\rm HP}$ based on Criterion 4 in different ranges of S. We find S of the companion planet in the system has a linear relation with the $P_{\rm HP}$ of an Earth-like planet in the HZ, as shown in the left panel of Figure 5. The point in the figure represents the $P_{\rm HP}$ of the specific range of S. Excluding the two outliers (green pentagrams), we can fit a linear relation between S and $P_{\rm HP}$ using the blue points. It turns out to be

$$P_{\rm HP} = -0.088 \log_{10} S + 0.922 \ . \qquad (10)$$

This correlation can be applied to estimate $P_{\rm HP}$ using the mass and period of another planet. However, besides the blue points in the left panel of Figure 5, two green points obviously deviate from the linear fitting. Both points have a much lower $P_{\rm HP}$ than the predicted value. The lower $P_{\rm HP}$ is mostly contributed by planets with very short periods ($<$40 d) and very large periods ($>$10 yr), which are hard to detect accurately. In the short-period case, the SNR decreases because the planet is close to the host star. Since the SNR is small, it is hard to detect the hot planet, whose signal is hidden as additional noise when we try to find the planet in the HZ. In the long-period case, motion of the star induced by the planet becomes approximately linear. Thus, it is hard to detect the other planet if the period is long enough. Consequently, the signal of planets in the HZ is hard to extract.

In the right panel of Figure 5, we show the relationship between the companion SNR and $P_{\rm HP}$. The planetary systems are from the two green points in the left panel. Most planets in systems with $S < 1$ have a semi-major axis larger than 10 AU. These planetary periods are far over 5 yr and the fitting program cannot find the planet properly. In this case, the influence of the signal from a planet is a small arc, but we can only fit the signal with a linear model that takes into account the proper motion term. The astrometry fitting residual is mainly from the differences between linear fitting of a small arc, which can be expressed as

$$A \approx 0.93 \ \mu{\rm as} \left(\frac{M_{\rm p}}{1 M_\oplus}\right) \left(\frac{a_{\rm p}}{1 {\rm AU}}\right)^{-2} \ . \qquad (11)$$

Most planets in systems with $5 < S < 7$ are short-period ($<$40 d) planets. The short-period planets' astrometry signal is calculated based on Equation (5) because it can finish the entire orbit in 5 yr. As we can see in Figure 5(b), the two dashed lines have an obvious decrease between SNR of 0.5 and 2. In this area, the signal of the companion planet is similar to the observational noise and can hardly be detected. Thus, $P_{\rm HP}$ decreases because the signal of the undetected planet makes the planet in the HZ hard to detect. In the case when SNR is small enough, the signal of the undetected planet is also small and limitedly influences the $P_{\rm HP}$, hence $P_{\rm HP}$ increases. The fitting results get worse when the signal of the companion planet is comparable with noise. For $P_{\rm HP} < 80\%$, the SNR of planets with $5 < S < 6$ is between 0.6 and 1.5, but $S < 1$ is between 1.6 and 2.0.

With knowledge of the companion planet's mass and period, using Equation (10), we can estimate $P_{\rm HP}$ of the planets in the HZ. Note, Equation (10) assumes that the SNR of the planet in the HZ is 10. Considering

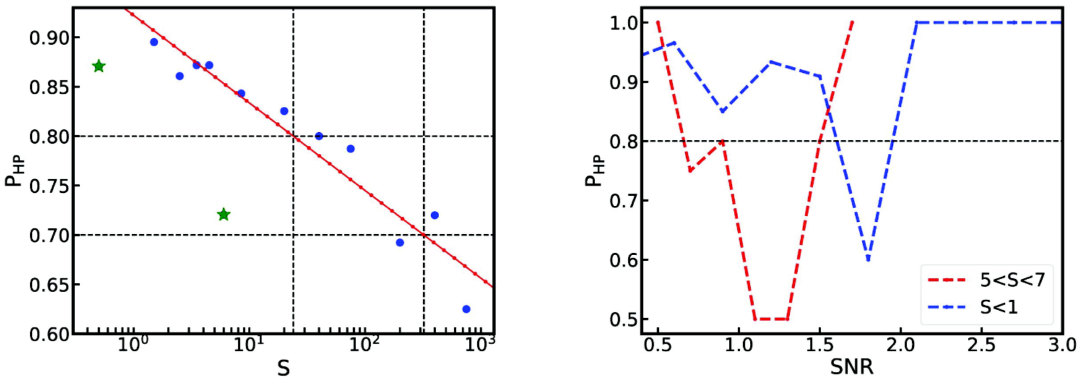

Fig. 5 The left panel is the relationship between $P_{\rm HP}$ and S. The *blue* and *green points* demonstrate that different S values lead to different $P_{\rm HP}$, with the same SNR (=10) of planets in the HZ. Excluding the two *green pentagrams* as outliers, the *red line* is the linear fitting of the *blue points* as shown in Equation (10). The right panel shows how the SNR of the companion planet (the X-axis) influences the $P_{\rm HP}$. In the range of $0.5 < \rm SNR < 2$, $P_{\rm HP}$ obviously decreases.

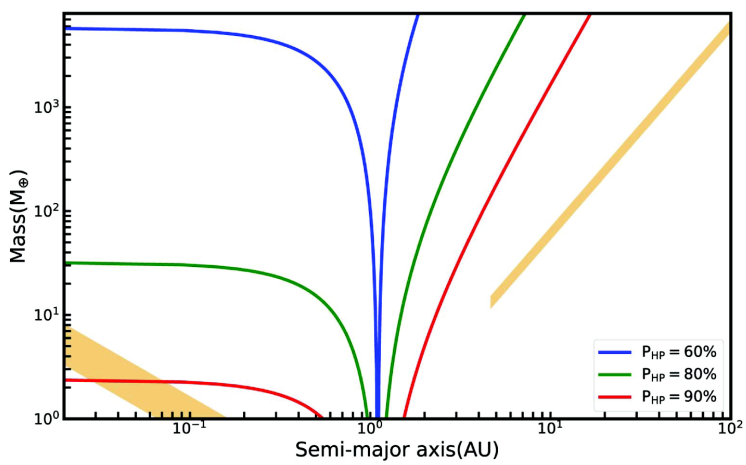

Fig. 6 Assuming an SNR for a planet in the HZ of 10, we estimate the influence of the companion planet. The *blue*, *green* and *red lines* represent the upper limits of the companion planet in different locations to achieve specific $P_{\rm HP}$ of 60%, 80% and 90% respectively. The *orange area* is the two special regions where the SNR of the companion planet is about 0.5–2. In these two regions, $P_{\rm HP}$ has an obvious reduction.

Equation (8), the $P_{\rm HP}$ can be expressed as

$$P_{\rm HP} \approx 1.20 \exp\left(-\frac{(K-1.20)^2}{0.325}\right) \times (-0.088 \log_{10} S + 0.922)\ . \tag{12}$$

Because $P_{\rm HP}$ cannot be larger than 1, the final result is the minimal value between 1 and the calculated one. Assuming the SNR of the planet in the HZ is 10, we calculate the different relationship between the mass of the companion planet M and its period T.

In Figure 6, we set the $P_{\rm HP}$ to be 90%, 80% and 60%. The red, green and blue lines indicate the respective companion planet's mass upper limits when plotted versus different semi-major axes. Only with mass below a specific line can we get a certain $P_{\rm HP}$. The orange area is the two dips we discuss in the right panel of Figure 4. The planetary systems in these two areas have P as low as 70%. For all the known nearby single planetary systems, we can estimate the parameters K and S. Using Equation (12), we can estimate $P_{\rm HP}$ if there is an additional Earth-like planet in the HZ. According to the estimated $P_{\rm HP}$, it is necessary to rank nearby planet hosts as possible targets for the *HEPS* mission.

4 DISCUSSION AND CONCLUSIONS

In this work, we are aiming to find suitable configurations of planetary systems that can be targeted by the future potential space mission *HEPS*. Using a simplified astrometric model of a star, we simulate the astrometric signals and develop a fitting program of planet parameters. Since multi-planet systems are much more common than single systems, we try to detect planets in the HZ of multi-planet systems. We define the detection probability $P_{\rm HP}$ to evaluate the detection probability of an Earth-like planet in the HZ, according to different criteria stated in Section 3. We set four criteria according to the fitting precision of the planet period, mass, eccentricity and inclination. To investigate the differences of $P_{\rm HP}$ between single and multi-planetary systems, we include another companion planet with different mass and location. The SNR of both planets will influence the detection of planets in the HZ according to Criterion 4.

In our simulations, all the host stars are fixed as solar-like stars with 1 solar mass at 10 pc. We find the SNR of the HZ is still one of the key factors influencing $P_{\rm HP}$. $P_{\rm HP} > 80\%$ requires the SNR>10. We fit $P_{\rm HP}$ as a function of SNR (Eq. 8). However, the SNR is not the only factor that influences detectability of the planets. The companion planet's mass and semi-major axis greatly influence $P_{\rm HP}$ even when Earth-like planets in the HZ have the same SNR. To describe the influence from companion planets, we define a parameter S depending on the parameters of both planets, as shown in Equation (9). By calculating $P_{\rm HP}$ with different S, we find a logarithmic negative correlation, as shown in Equation (10). However, we find two dips in Figure 4, where the SNR of the companion planet is between 0.5 and 2. Because we cannot detect the companion planets in these two regions, the signal of the companion planets is considered as noise when fitting the planet in the HZ. Therefore, the SNR of the planet in the HZ reduces and $P_{\rm HP}$ decreases. As an extended conclusion, an Earth-like planet in the HZ is harder to detect ($P_{\rm HP} < 80\%$) in a system with a hot Jupiter or warm Jupiter (typically within 2 AU). Considering both SNR and influence from the companion planet simultaneously, we estimate an approximation of $P_{\rm HP}$, as shown in Equation (12).

The crucial reason why another planet influences the detection of a planet in the HZ is the degeneracy of the large number of parameters. The fitting residuals of the first planet will contaminate the small signal of the planet in the HZ. In the case of a solar system at 10 pc, Jupiter generates an astrometric signal of $\sim$5 mas, while the signal induced by Earth is only 0.3 μas. Thus, the fitting parameter of Jupiter must be very precise to ensure the residuals will be smaller than the signal from Earth. Especially when the first planet is not detected, the detection probability of the planet in the HZ obviously decreases. Combining data via transiting or radial velocity, we can improve the detection probability and accuracy of fitting parameters for the first planet, thus enhancing $P_{\rm HP}$.

Our work here is based on the two-planet systems we simulate. Real multi-planet systems containing more than two planets have a much larger parameter space. The influences from the companion planets are much more complicated than two planet systems. Besides the SNR of the planet in the HZ, we show that the negative correlation between S and $P_{\rm HP}$ is another major characteristic. In the next work, we will test the relationship we find here in detecting planet systems and rank detection probabilities of Earth-like planets in the HZ around all the nearby planet hosts.

Acknowledgements This work is supported by the National Natural Science Foundation of China (Grant Nos. 11503009, 11333002 and 11673011). We also thank the Heising-Simons Foundation, the Fundamental Research Funds for the Central Universities (Nos. 14380018 and 14380023) and the Technology of Space Telescope Detecting Exoplanet and Life supported by the National Defense Science and Engineering Bureau civil spaceflight advanced research project D030201.

References

Anglada-Escudé, G., Amado, P. J., Barnes, J., et al. 2016, Nature, 536, 437

Bakos, G. Á., Noyes, R. W., Kovács, G., et al. 2007, ApJ, 656, 552

Burke, C. J., Christiansen, J. L., Mullally, F., et al. 2015, ApJ, 809, 8

Casertano, S., Lattanzi, M. G., Sozzetti, A., et al. 2008, A&A, 482, 699

Chen, D., Wu, J., & Li, B. 2013, European Planetary Science Congress, 8, EPSC2013

Fehlberg, E. 1968, Classical Fifth-, Sixth-, Seventh- and Eighth-Order Runge-Kutta Formulas with Stepsize Control, Tech. rep., NASA Tech. Rep. No. 287, Huntsville

Gillon, M., Triaud, A. H. M. J., Demory, B.-O., et al. 2017, Nature, 542, 456

Henry, T., Dieterich, S., Finch, C., et al. 2018, in American Astronomical Society Meeting Abstracts, 231, 349.17

Howard, A. W., Johnson, J. A., Marcy, G. W., et al. 2011, ApJ, 730, 10

Kopparapu, R. K., Ramirez, R., Kasting, J. F., et al. 2013, ApJ, 765, 131

Liu, H.-G., Jiang, P., Huang, X., et al. 2018, AJ, 155, 12

Malbet, F., Goullioud, R., Lagage, P.-O., et al. 2012, in Proc. SPIE, 8442, Space Telescopes and Instrumentation 2012: Optical, Infrared, and Millimeter Wave, 84420J

Marquardt, D. W. 1963, Journal of The Society for Industrial and Applied Mathematics, 11, 431

Miralda-Escudé, J. 2002, ApJ, 564, 1019
Montenbruck, O., & Gill, E. 2012, Satellite Orbits: Models, Methods and Applications (Springer Science & Business Media)
Pepe, F., Lovis, C., Ségransan, D., et al. 2011, A&A, 534, A58
Perryman, M., Hartman, J., Bakos, G. Á., & Lindegren, L. 2014, ApJ, 797, 14
Schödel, R., Ott, T., Genzel, R., et al. 2002, Nature, 419, 694
Udry, S., Dumusque, X., Lovis, C., et al. 2017, arXiv:1705.05153
Unwin, S. C., Shao, M., Tanner, A. M., et al. 2008, PASP, 120, 38
van Leeuwen, F. 2007, A&A, 474, 653
Wittenmyer, R. A., Wang, S., Horner, J., et al. 2013, ApJS, 208, 2
Wright, J. T., & Howard, A. W. 2009, ApJS, 182, 205
Xie, J.-W. 2013, ApJS, 208, 22
Yang, M., Liu, H.-G., Zhang, H., Yang, J.-Y., & Zhou, J.-L. 2013, ApJ, 778, 110
Zechmeister, M., & Kürster, M. 2009, A&A, 496, 577